Journal of Metals, Materials and Minerals, Vol. 33, No. 1, pp. 65-72, 2023

Investigating the effect of temperature and NaCl concentration on corrosion behavior using commercial food cans

Samar S. HUSSEIN[1], Abeer A. RADHI[1], and Wafaa K. MAHMOOD[1,*]

[1] *Department of Production Engineering and Metallurgy, University of Technology-IRAQ, Baghdad, IRAQ*

***Corresponding author e-mail:** wafaa.k.mahmood@uotechnology.edu.iq

Received date:
7 September 2022
Revised date
27 December 2022
Accepted date:
29 December 2022

Keywords:
Corrosion;
Food cans;
Tin-plate;
Chloride acid

Abstract

In the present work, commercial tin-plate used as storage cans for three different products (salmon fish, green peas, and corn) are used to investigate the corrosion to storage temperature and salt concentration. The corrosion process was electrochemically monitored using the potentiodynamic polarization method and the structure and concentrations of the corrosion products were investigated using X-ray diffraction (XRD). To characterize the resulting sample morphology, emission scanning electron microscopy (FESEM) was used. The results showed that the corrosion resistance of the tin-coating, was important constant and by changing the NaCl concentration and operation temperature, the corrosion resistance was lower. It is believed that the steel substrate dissolution that is underneath the tin coating is the main driving force for the investigated corrosion process. The experimental results show that the operating temperature has a higher impact on the corrosion rate because it promotes a heavy tendency on the rate of diffusion of molecules or ions in a solution. Green peas tin-plates are corroded more than corn, and salmon fish tin-plates when the temperature was increased from 25°C to 50°C and showed higher negative corrosion potential and higher corrosion current density in sodium chloride solutions.

1. Introduction

Tin-plate is made of carbon-steel thin sheets coated from all sides by electrolytic tin. This coated sheet can combine two important properties which are the strength of the steel and the corrosion resistance offered by the tin layer [1-3]. The tin layer usually acts as a sacrificial anode that resists galvanic corrosion by oxidant agents in the stored products like food by preventing the formation of oxides on the can's internal surface [4,5]. Tin-plate is widely used in the packaging and storage in the food and beverage industries beside other important industrial fields like aerosol containers, wax, paints, chemicals, and many other fields [5-9].

Despite the wide usage of tin-plate in the mentioned industrial fields, it still suffers from several drawbacks that in many cases have an impact on the stored products themselves such as corrosion [10-12]. Tin-plate corrosion may take different forms depending on the stored product, in many cases pitting corrosion that happens when ion dissolution happens at coating fractures, stress corrosion, and sulfide black corrosion [13-17].

Large numbers of studies have been performed to understand the corrosion-controlling mechanisms in the tin-plate and most of these studies focused on investigating the corrosion behavior of pure tin plates [18,19]. It is believed that the nature of electrolytes associated with canned food is a major factor in determining the corrosion resistance and mechanism of any tin-plate [20]. Tselesh [21] and Refaey and Schwitzgebel [22] investigated the anodic behavior of tin and they showed that the presence of citrate buffer solution can result in passive-active transitions during the process. Jafarian *et al.* [23] used sodium carbonate solution in the absence of the iodide and chlorin solutions and they found that the behavior is similar to that reported by Refaey and Schwitzgebel [22] while Huang *et al.* [14] investigated the effect of sodium hydroxide solution and they concluded that the passive-active transition is the controlling anodic behavior during the storage process. Tin-plate is used to protect the tin carbon-steel sheet from corrosion when acting as a sacrificial anode but on the other hand, the tin-plate is corroding as well. One of the important factors that have been investigated by several researchers is the effect of NaCl on the whole corrosion process in tin plates. The corrosion behavior of tin-plate will be investigated for different types of canned foods with NaCl concentration for each canned food under different storage temperatures by using a polarization curve and determining the type of cans that increases the corrosion rate with different operation conditions (temperature or concentration). The morphology of the corroded tin-plate was observed by field emission scanning electron microscopy, and the composition of the coating surface before and after corrosion was investigated using X-ray diffraction.

2. Experimental

2.1 Materials

The tin-plate sheets used in this work were collected from commercial food cans in the local supermarkets and were purchased from the same manufacturer for corn, green peas, and salmon packing

DOI: 10.55713/jmmm.v33i1.1595

to avoid the differences in the tin-plate grades. The tin plate was made of a low carbon steel base with a thickness of 0.4 mm that had been electrodepositively coated with tin on both sides, with a thickness of roughly (3 µm), and the composition of carbon steel base for cans as shown in Table 1. A sample from each can with dimensions (10 mm × 10 mm) was cleaned with ethanol and dried before being exposed to NaCl solution. The percentage of sodium chloride in each can was 0.651 $g \cdot L^{-1}$ for the salmon can, 4.5 $g \cdot L^{-1}$ for the corn can, and 12.38 $g \cdot L^{-1}$ for the green peas can. In this paper, a symbol is given to each sample after the immersion test as shown in Table 2.

2.2 Electrochemical measurements

The potentiodynamic polarization was carried out using an electrochemical cell and Versa Studio control software. A three-electrode system with the tin-plate with an exposed area of 1 cm^2 as the working electrode (WE), a saturated calomel electrode as the reference electrode (RE), and a commercial ruthenium-titanium electrode as the counter electrode (CE) was used. The samples were exposed to (0.651 $g \cdot L^{-1}$, 4.5 $g \cdot L^{-1}$, 12.38 $g \cdot L^{-1}$) NaCl solution at the temperature of (25°C, 35°C, and 50°C) and were obtained by using a biochemical incubator to simulate the different storage temperatures during the transportation and storage process of canned food. Open circuit potential (OCP) and Tafel polarization techniques were used. After 30 min of immersion, the polarization curve of tin-plate in citric acid solution was conducted at a scan rate of 0.1667 $mV \cdot s^{-1}$, and the corrosion potential E_{corr} and corrosion current density I_{corr} were calculated and obtained. At a scanning rate of 0.1667 $mV \cdot s^{-1}$, the potentiodynamic polarization tests were carried out.

2.3 Immersion test

Tin-plate samples with the dimension of 10 mm × 10 mm were immersed in (0.651 $g \cdot L^{-1}$salmon, 4.5 $g \cdot L^{-1}$ corn, and 12.38 $g \cdot L^{-1}$ green peas) NaCl solution at the temperature of 25°C, 35°C, and 50°C for 30 min. The corroded samples were removed from the solution after immersion times and cleaned with distilled water and ethanol. The surface morphology corroded surface of tin-plate was observed by field emission scanning electron microscopy (FESEM). The composition of the coating surface with different colors for canned food (white and gold color) before corroding and the corroded surface were analyzed by X-ray diffraction (XRD).

Figure 1 shows the flow diagram of the experimental work.

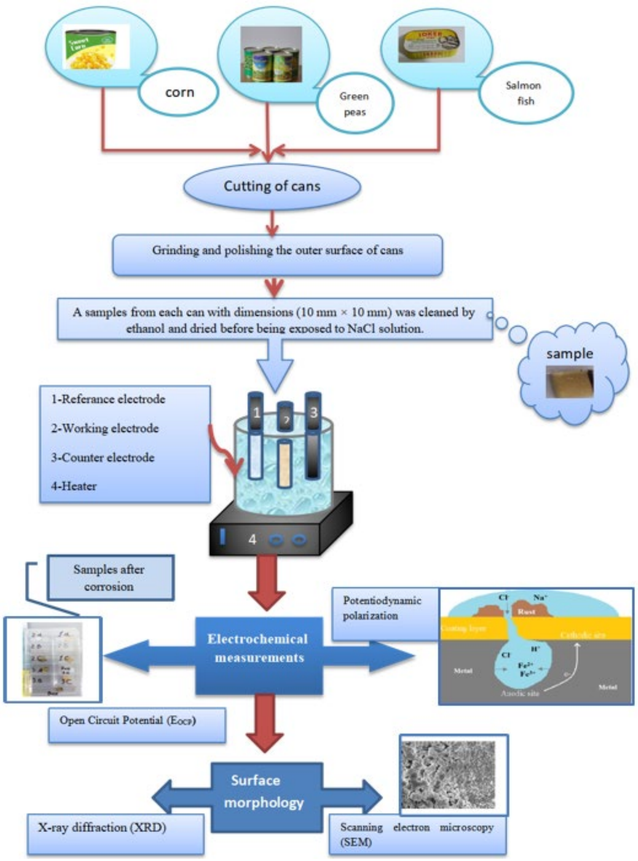

Figure 1. schematic diagram of the working steps.

3. Results and discussion

3.1 Corrosion behavior (potentiodynamic polarization)

3.1.1 Open circuit potential (EOCP)

Figure 2 shows the variation for E_{OCP} as a function of immersion time (30 min). It is important to highlight that each can plate was tested with the salt concentrations associated with it as it was taken from the local market and the solution salinity was not controlled. At each temperature and for all studied NaCl solution concentrations, the potential disturbance and instability occur at ambient temperature (25°C) while much more stable potential readings were spotted at the other experimented temperatures (35°C and 50°C). Testing the

Table 1. The chemical composition of the carbon steel base.

Elements	Fe	Al	Mo	Cr	Ni	Cu	P	Mn	Si	S	C
Weight (%)	Rest	0.3	0.05	0.1	0.16	0.2	0.03	0.34	0.03	0.03	0.08

Table 2. the symbols of tin-plate cans.

Temperature	Type of food cans		
	Green peas cans (12.38 $g \cdot L^{-1}$ NaCl)	Corn cans (4.5 $g \cdot L^{-1}$ NaCl)	Salmon fish cans (0.651 $g \cdot L^{-1}$ NaCl)
25°C	1a	2a	1a
35°C	1b	2b	1b
50°C	1c	2c	1c

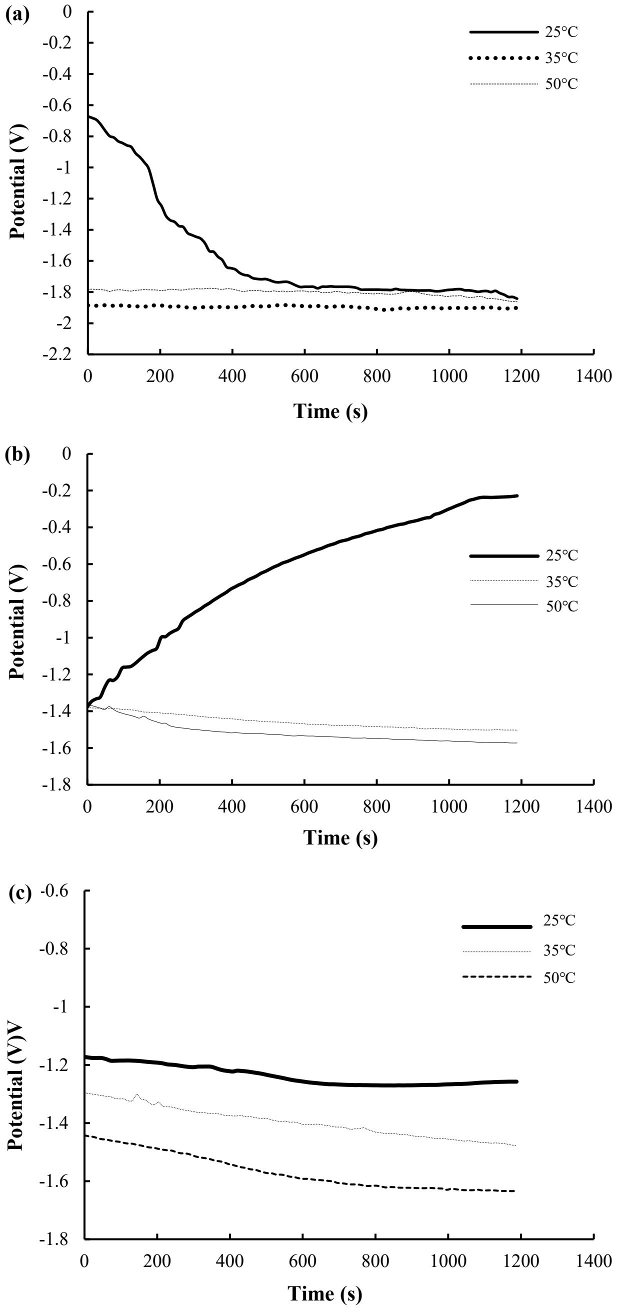

Figure 2. Open Circuit Potential (OCP) for different types of canned (a) Salmon fish, 0.651 g·L^{-1} (b) corn, 4.5 g·L^{-1}, and (c) green peas, 12.38 g·L^{-1} at different temperatures.

Salmon fish can plates show that, all the measured potential values are within the range of -1.9 V to -1.8 V and only slight variations in values and no variation correlation between E_{OCP} and temperature. This behavior is due to the increment in the potential of anodic polarization at 0.651 g·L^{-1} NaCl concentration which resulted in decreasing the corrosion rate. For higher sodium chloride solution (as in the corn cans (4.5 g·L^{-1})), the corn can's plate potential value shifts in the negative direction, typically decreasing from -1.265 V (25°C) to -1.504 V (35°C) and -1.573 V (50°C). In the case of the green peas can plates with a salinity of 12.38 g·L^{-1}, the potential value shifts in the negative direction from -1.232 V (25°C) to -1.491 V (35°C) and -1.38V (50°C) respectively. It is worth noting that, the final OCP values decrease exponentially with increasing concentration. This behavior is due to the increment in the transpassive potential that is usually caused by the increment in the NaCl concentration which results in a clear decrease in the corrosion rate. Generally, it is believed that the passive and transpassive potential of green peas in the anodic polarization region decreases by increasing the temperature and concentration.

3.1.2 Potentiodynamic polarization

The polarization parameters are summarized in table (1) where the corrosion parameters include the corrosion current density (I_{corr}), potential (E_{corr}), and Tafel slopes (β_a and β_c), which are presented as a function of temperature and NaCl solution concentration. The corrosion current density and corrosion potential were obtained using the linear extrapolation of Tafel. In this study, the polarization curve is fitted by selecting the straight line of the cathodic and anodic curve region beyond 50 mV above and below the corrosion potential to ensure that in the strong polarization region. From Table 3 the corrosion rate of tin-plate increases by increasing the NaCl concentration and temperature. The green peas tin plate showed a higher corrosion rate when compared to the corn and salmon fish tin plates due to the dissolution of the tin coating, formation of corrosion products, and the presence of corrosion pits.

Figure 3 shows Potentiostatic polarization curves for salmon fish canned in 0.651 g·L^{-1} sodium chloride solution at different temperatures. It is clear that the temperature has a minor effect on the corrosion potential which agrees with the results reported by Urbano *et al.* [24]. On the other hand, the results showed that the corrosion current density (I_{corr}) increases by increasing the temperature. The polarization curve of tin-plate in 0.651 g·L^{-1} sodium chloride solution is a higher polarization

Table 3. Corrosion current density and potential of different canned food in NaCl acid solution at one concentration for each canned at different temperatures.

Type of canned food	Temp. (°C)	OCP (V)	E (I=0) (mV)	Icorr (µA)	Bc (mV)	Ba (mV)	CO. Rate (mmpy)
Salmon fish (0.651 g·L^{-1})	25	-1.902	-893.719	1.0411	149.173	146.547	0.1533
	35	-1.875	-839.560	1.744	73.219	79.387	0.4726
	50	-1.884	-846.785	3.540	72.340	82.970	0.2608
Corn (4.5 g·L^{-1})	25	-1.265	-561.122	1.5285	143.537	147.272	0.1973
	35	-1.504	-692.199	17.919	65.647	50.632	1.157
	50	-1.573	-726.408	12.2806	163.860	81.116	2.918
Green peas (12.38 g·L^{-1})	25	-1.232	-567.373	1.035	189.798	179.366	0.1524
	35	-1.491	-632.244	20.357	123.901	75.019	1.4995
	50	-1.638	-714.948	12.1254	170.729	85.626	3.2855

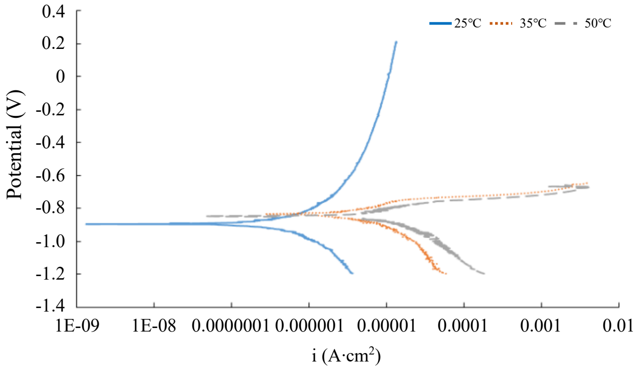

Figure 3. Potentiostatic polarization curves for salmon fish canned in 0.651 g·L^{-1} sodium chloride solution at different temperatures.

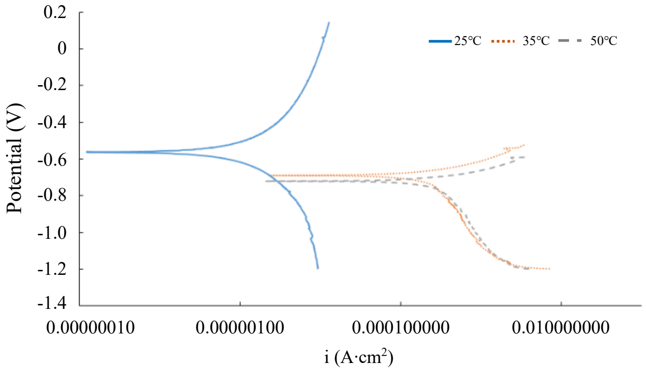

Figure 4. Potentiostatic polarization curves for corn canned in 4.5 g·L^{-1} sodium chloride solution at different temperatures.

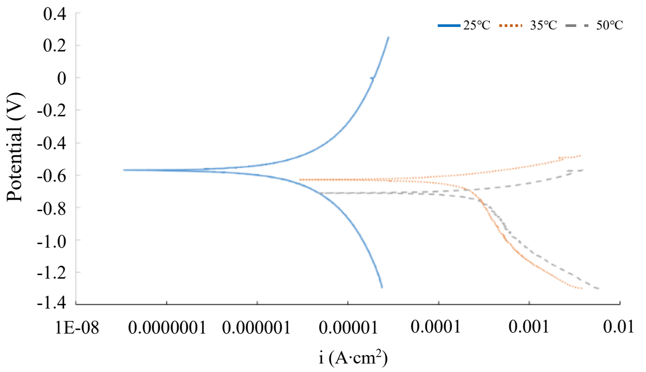

Figure 5. Potentiostatic polarization curves for green peas canned in 12.38 g·L^{-1} sodium chloride solution at different temperatures.

current, and due to the diffusion of dissolved oxygen, a polarization platform is found in the cathodic region. The corrosion current density of tin-plate in 0.651 g·L^{-1} NaCl solution is 1.0411 µA.cm^{-2}, 1.744 µA.cm^{-2}, and 3.54 µA.cm^{-2} at 25, 35, and 50°C respectively, showing that the presence of oxygen does promote the corrosion of tin in NaCl solution.

Figures 4 and 5, show the polarization curves of corn and green peas canned in 4.5 g·L^{-1} and 12.38 g·L^{-1} NaCl solutions respectively, and at different temperatures. It can be observed from Figure 4 that the corrosion potential of tin-plate declined from -0.567373 V (25°C) to -0.632244V (35°C) and -0.714948 V (50°C) with increased temperature. which indicates that the surface activity of tin-plate (green peas) increases with the presence of more Cl$^-$ ions, thus green peas can be more disposed to corrosion. The figures show that the polarization curve starts from a relatively negative reduction potential causing the value of the corrosion potential to be slightly lower than the final E$_{OCP}$ at the same concentration. At higher salt concentrations the E_{corr} is shifted to be negative which is compatible with the decrease of final E$_{OCP}$.

At 35°C, it was observed that there is a more corrosion potential E_{corr} in a high salt solution, it inclines from -839.56 mV in 0.651 g·L^{-1} to -692.199 mV in 4.5 g·L^{-1} and -632.244 mV in 12.38 g·L^{-1}. However, increasing the concentration causes the corrosion current density i_{corr} to increase. It rises from 1.744 µA.cm^{-2} in 0.651 g·L^{-1} to 17.919 µA.cm^{-2} in 4.5 g·L^{-1} and 20.357 µA.cm^{-2} in 12.38 g·L^{-1}, which indicates that canned green peas have a higher corrosion rate at 12.38 g·L^{-1}, due to the presence of more aggressive Cl$^-$ ions that can expedite the dissolution of electrochemical.

The Tafel slopes (β_a & β_c) are affected by the concentration changes. When the salinity of a solution increases, anodic tafel slope β_a decreases, which indicates that the concentration of sodium chloride increases in Cl$^-$ ions and is useful to the anode reaction. Deterioration in the passive film on the surface, and reduction in the protective property, that the anodic oxidation is accelerated. Meanwhile, β_c decreases when the concentration of sodium chloride solution increases, which indicates that the increasing sodium chloride influence the cathode reaction. The presence of more Na$^+$ and Cl$^-$ in the solution will certainly increase the conductivity of the electrolyte. The reaction current path is prolonged due to the strong solution conductivity which leads to the fact that the charge created by the anodic oxidation reaction on the surface of the electrode is consumed by the redox reaction further away from the surface. In other words, an increase in the region that can support oxygen reduction due to increased conductivity, and thus leads to an increase in the reduction current of oxygen, eventually the cathodic reaction rate increase.

3.2 Surface morphology

The surface morphology of tin-plate cans before and after immersion test in NaCl g·L^{-1} solution at various temperatures is shown in Figure 6. Figure 6 shows the FESEM image of green peas tin-plate, corn, and Salmon fish for (1, 2, and 3) respectively after being exposed to NaCl solution for 30 min. Tin-plate cans' surfaces were clean and free of corrosion agents before exposure. A barrier layer like plates at 25°C was the formation by the increase in NaCl concentration of (1a) than (2a) and (3a) which was observed by a decrease in the corrosion rate of (1a) compared with (2a) and (3a) at 25°C as shown in Table 3. Above 3% NaCl, the continuing decreased solubility of oxygen becomes more important than any change in the diffusion that is a barrier layer, hence, the corrosion rate decrease. (R. Winston Revie *et al.*, 2008). At (25°C) (Figure 6(1a)) some porous corrosion scale with embedded crystals, possibly of corrosion products was observed. The presence of chloride ions will substantially decrease the ability of the passive film to negative metal oxidation or dissolution. Corrosion products like particulates were observed on the surface (35°C) (Figure 6(1b)). As temperature increases to 50°C.

- The increased temperature and negative charge of the chloride ion penetrate through the coating to the positively charged metal cation destroying the protective function of the tin coating and increasing the dissolution rate of iron.

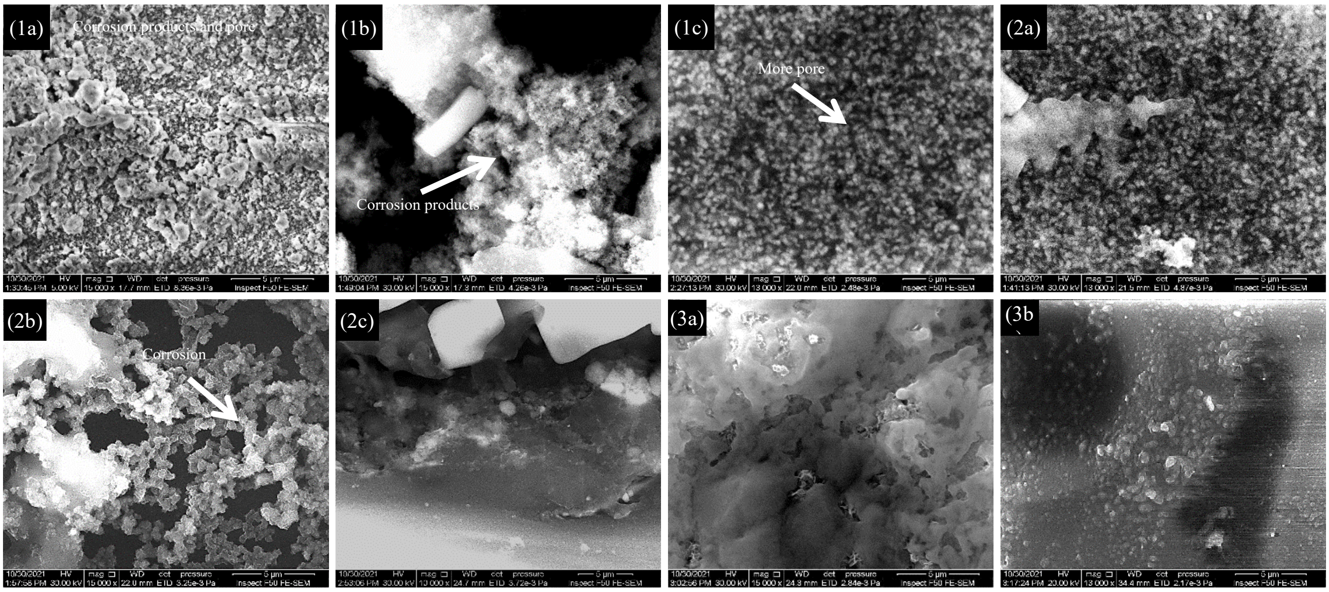

Figure 6. FESEM surface morphology of tin-plate after immersion test in NaCl solution for green peas (1a,1b,1c) in 12.38 g·L^{-1} NaCl at (25, 35, and 50°C), (2a, 2b, 2c) image for corn (4.5 g·L^{-1} NaCl) at (25, 35, and 50°C), and (0.651 g·L^{-1} NaCl) for salmon fish tin-plate at (25°C and 50°C) respectively

Table 3. Corrosion current density and potential of different canned food in NaCl acid solution at one concentration for each canned at different temperatures.

Type of canned food	Temp. (°C)	OCP (V)	E (I=0) (mV)	Icorr (μA)	Bc (mV)	Ba (mV)	CO. Rate (mmpy)
Salmon fish (0.651 g·L^{-1})	25	-1.902	-893.719	1.0411	149.173	146.547	0.1533
	35	-1.875	-839.560	1.744	73.219	79.387	0.4726
	50	-1.884	-846.785	3.540	72.340	82.970	0.2608
Corn (4.5 g·L^{-1})	25	-1.265	-561.122	1.5285	143.537	147.272	0.1973
	35	-1.504	-692.199	17.919	65.647	50.632	1.157
	50	-1.573	-726.408	12.2806	163.860	81.116	2.918
Green peas (12.38 g·L^{-1})	25	-1.232	-567.373	1.035	189.798	179.366	0.1524
	35	-1.491	-632.244	20.357	123.901	75.019	1.4995
	50	-1.638	-714.948	12.1254	170.729	85.626	3.2855

- At (4.5 g·L^{-1} NaCl for corn cans) Figure 6(2a) and XRD data that the corrosion product is composed of Fe content was high at (25°C), showing more pore formation by corrosion products are composed of high Fe contents at (25°C) and like the flower of corrosion products at 35°C Figure 6(2b), while (0.651 g·L^{-1} NaCl salmon fish cans) at (25°C) observed cloud shape of corrosion products results of oxides was formation Figure 6(3a) and XRD data. This observation is due to the increase in the potential of anodic polarization region at 0.651 g·L^{-1} NaCl concentration mean decrease in the formation of insoluble Sn corrosion products with the formation of cloud shape of corrosion products and provide less corrosion rate but at 4.5 g·L^{-1} NaCl decrease in the potential of anodic polarization and formation of Sn and Fe with pitting formation means corrosion products does not provide protective nature at 25°C.

As the temperature increases from 35°C to 50°C, the corrosion of tin-plate and pit formation in NaCl solution is higher than that observed in the 0.651 g·L^{-1} NaCl salmon fish cans. The corrosion products like flakes presented in Figure 6(3c) at 50°C are corrosion of salmon fish tin-plate in NaCl solution mostly by the dissolution of steel substrate. Flow-independent corrosion is a consequence of a diffusion barrier created by the magnetite scale, present only at high temperatures and low NaCl concentration as shown in Figure 6(3b).

3.3 X-ray diffraction (XRD) analyses

The crystal structure of all the investigated cans was characterized using an X-ray diffractometer. The phases of NaCl, FeO, and FeOOH can be identified by the samples' diffraction peaks. The results reviled NaCl traces on the tin-plate surface due to the presence of more aggressive Cl$^-$ ions that tin-plate can corrode the tin coating and steel substrate with a change in temperature and more formation of corrosion products (tin and steel materials). Iron was the main corrosion product which indicates that it was the main driving force for corrosion, (the dissolution of steel substrate underneath the tin coating). Steels that have been exposed to the atmosphere for several years develop an inner black protective layer and an exterior red rust layer as protective oxides. The protective properties of the layer that developed on the surface of metal after a specific type of oxidation are thought to be related to the passive film's crystal structure. As a result of metals' interactions with water, oxide or hydroxide coatings have formed, which is what gives metals their anodic passivity. The anodic passive film contains a high concentration of point defects such as metal vacancies, electrons, and holes (Sami *et al.,* 2014). Increasing temperature has a heavy tendency to the rate of the diffusion of molecules or ions in a solution, even if it makes oxygen less soluble in water.

The corrosion films shown in Figure 7(1a) for pure tin-plate exposed to NaCl solution were composed of SiO_2, Fe_2O_3, Al_2O_3, and $FeCl_3$ at 2θ values (30.7648°, 49.8452°, 27.5411°, and 54.9452°) respectively. These corrosion products were detected on the 1c tin-plate SiO_2, Fe_7O_9, Fe, $FeCl_3$, and Al_2O_3 with 2θ values of (65.0607°, 27.4614°, 44.7080°, 36.0850°, and 54.3493°) respectively. Figure 7(1c) indicates that the quantity of corrosion products of (1c) was possibly so high with $FeCl_2$ and the Fe compounds content was found to increase, which indicates that the corrosion products primarily were iron oxide. Figure 7(2a) shows that the concentration of tin oxide was 0.4% when immersed in 4.5% NaCl solution $Fe(OH)_2$, FeO, and SnO_2 at values of 2θ (27.4614°, 65.1025°, and 54.4283°) respectively. The compounds of iron ions shown in Figure 6(2c) are larger than that shown in Figure 7(1a) sample under the same temperature (Fe_7S_8, Fe, and SnS) with 2θ values of (64.9887°, 44.6685°, and 32.9429°) respectively. These results show that the corrosion of (1a and 1c tin-plate samples) in NaCl solution is mainly by the formation of steel corrosion products without Sn compounds meaning dissolution of the steel substrate and more pitting formation, whereas the corrosion products of tin are predominated in the corrosion of 2a and 2c tin-plate samples in NaCl solution was observed fewer pits in Figure 7.

For the Salmon fish cans samples (0.651 $g\cdot L^{-1}$ NaCl, and 25°C), the corrosion product of Figure 6(3a) is composed by (Al_2O_3, Fe, SiO_2) at 2θ values of 64.9938°, 78.0667°, and 44.7061° respectively. At 50°C and 0.651 $g\cdot L^{-1}$ NaCl for Salmon fish cans samples Figure 7(3c), the 2θ of (Al_2O_3 and SiO_2) is 64.8732°, and 77.9404° respectively. The Fe_3O_4 is formed at (5.4%) and 2θ (31.7539°) which indicates that the corrosion rate of salmon fish cans at 0.651 $g\cdot L^{-1}$ concentration and 50°C in NaCl solution is decreased due to the dissolution of steel substrate and formation of magnetite, aluminum oxide, and silicon oxide. The phases and quantities analysis of cans samples by using the match program as shown in Table 4.

Table 4. The phases and quantities analysis of tin-plate cans.

Symbol of samples	Phases analysis	Quantities analysis (%)
1a	SiO_2	77.4%
	Fe_2O_3	13.3%
	Al_2O_3	4.9%
	$FeCl_3$	4.4%
1c	SiO_2	61.2%
	Fe_7O_9	15.7%
	Fe	14.3%
	$FeCl_3$	5.4%
	Al_2O_3	3.3%
2a	$Fe(OH)_2$	21.5%
	FeO	16.9%
	SnO_2	0.4%
2c	Fe_7S_8	24.7%
	Fe	15.7%
	SnS	5%
3a	Al_2O_3	43.2%
	Fe	23.2%
	SiO_2	18.2%
3c	Al_2O_3	48.2%
	SiO_2	39.6%
	Fe_3O_4	5.4%

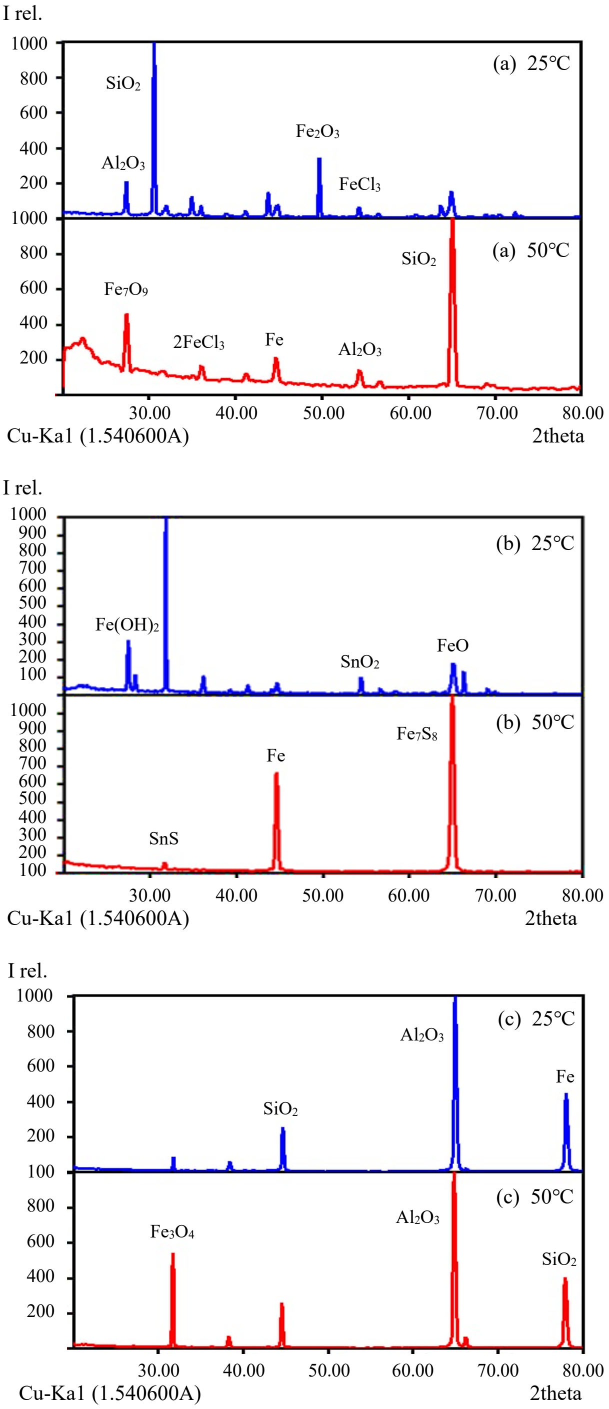

Figure 7. X-ray diffractometer results of the tested samples: (a) green peas cans at 25°C and 50°C, (b) corn cans at 25°C and 50°C, and (c) salmon fish cans at 25°C and 50°C.

The experimental results of the present work indicated that the electrochemical activity of the canned food surface is increased due to the presence of Cl^- ions. The dissolution of canned is accelerated and increases in the corrosion current density when the concentration of NaCl solution increase, this is, due to the deterioration of the passivation film on its surface and the promotion of the electrochemical reaction. With the increase in temperature from 25°C to 50°C, canned food has a more negative corrosion potential and higher corrosion current density in sodium chloride solutions. Green peas tin-plates are corroded more than corn, and salmon fish tin-plates with increased temperature, indicating that the presence of more chloride ions increases the surface activity of the tin-plate (Green peas), thus Green Peas canned are more susceptible to corrosion. increasing the temperature will promote a heavy tendency on the rate of diffusion of molecules or ions in a solution, which indicates the temperature is the main cause of corrosion more than NaCl concentration.

3.4 Mechanism of pitting corrosion

The mechanism of pitting corrosion generally consists of two stages during the metal dissolution process. The pit initiation stage is the product of the electrochemical activity of the canned food surface exposed to aggressive ions (Cl^-). And the pit propagation stage is progress autocatalytically and produces cavities at the surface. However, depends on the electrolyte, the microstructure of the material, and various electrochemical factors. The presence of Chloride ions (Cl^-) are responsible for pit corrosion on carbon steels as shown in Figure 8 according to Equation (1-10). Where electrons flow from the anodic site (carbon steel) to the cathodic side (Oxygen on the surface).

Anodic reactions:

$$3Fe + 4H_2O \rightarrow Fe_3O_4 + 8H^+ + 8e^- \quad (1)$$

$$Fe \xrightarrow{\text{dissolution}} Fe_2^+ + 2e^- \quad (2)$$

$$Fe_2^+ + H_2O \xrightarrow{\text{hydrolyses}} FeOH^+ + H^+ \quad (3)$$

$$3FeOH^+ + H_2O \xrightarrow{\text{oxydation and precipitation}} Fe_3O_4 + 5H^+ + 2e^- \quad (4)$$

The hydrolysis of Fe^{2+}, Fe^{3+} is accelerated in the presence of Cl^-, as shown in Equation (5-8);

$$Fe_2^+ + Cl_2^- \xrightarrow{\text{hydrolyses /chlorination}} FeCl_2 \quad (5)$$

$$FeCl_2 + H_2O \rightarrow FeOH^+ + H^+ + 2Cl^- \quad (6)$$

$$Fe_2^+ + H_2O \rightarrow FeOH^+ + H^+ \quad (7)$$

$$FeOCl \xrightarrow{\text{solidstate /precipitation}} FeOOH \quad (8)$$

Cathodic reaction:

The electrons flow to the cathode (passivated surface) are discharged in the cathodic reaction:

$$\tfrac{1}{2}O_2 + H_2O + 2e^- \leftrightarrow 2OH^- \quad (9)$$

$$2H^+ + 2e \rightarrow H_2 \quad (10)$$

High concentrations of chloride ions within corrosion pits produce pit propagation consistent with anodic dissolution by diffusion.

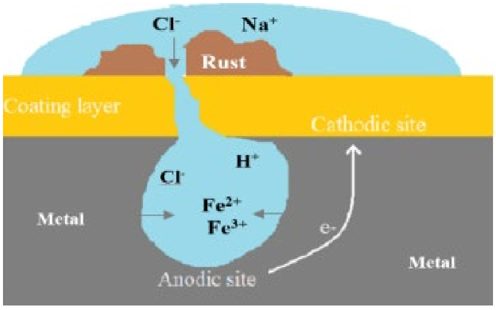

Figure 8. Chloride attack on carbon steel.

4. Conclusions

The experimental results of the present work indicated that the electrochemical activity of the canned food surface is increased due to the presence of Cl^- ions. The dissolution of canned is accelerated and increases in the corrosion current density when the concentration of NaCl solution increase, this is, due to the deterioration of the passivation film on its surface and the promotion of the electrochemical reaction. With the increase in temperature from 25°C to 50°C, canned food has a more negative corrosion potential and higher corrosion current density in sodium chloride solutions. Green peas tin-plates are corroded more than corn, and salmon fish tin-plates with increased temperature, indicating that the presence of more chloride ions increases the surface activity of the tin-plate (Green peas), thus Green Peas canned are more susceptible to corrosion. increasing the temperature will promote a heavy tendency on the rate of diffusion of molecules or ions in a solution, which indicates the temperature is the main cause of corrosion more than NaCl concentration.

Acknowledgements

The authors wish to acknowledge the unlimited financial and scientific support of the University of Technology-IRAQ that contributed significantly to accomplishing this work.

References

[1] Y. Xia, S. Zhang, L. Tong, S. Liu, G. Lin, Z. Bai, Y. He, and Z. Liu, "Introducing cyano-functionalized multiwalled carbon nanotubes to improve corrosion resistance and mechanical performance of poly(arylene ether nitrile) coating," *Surface and Coatings Technology*, vol. 432, p. 128058, 2022.

[2] Y. Chen, W. Bai, J. Chen, X. Chen, J. Zhao, F. Wei, R-K. Jian, X. Zheng, and Y. Xu,"In-situ intercalation of montmorillonite/urushiol titanium polymer nanocomposite for anti-corrosion and anti-aging of epoxy coatings," *Progress in Organic Coatings*, vol. 165, p. 106738, 2022.

[3] F. Su, X. Du, T. Shen, A. Qin, and W. Li, "Aggregation-induced emission luminogens sensors: Sensitive fluorescence 'Turn-On' response for pH and visually chemosensoring on early detection of metal corrosion," *Progress in Organic Coatings*, vol. 153, p. 106122, 2021.

[4] H. Zheng, W. Liu, S. He, R. Wang, J. Zhu, X. Guo, N. Liu, R. Guo, and Z. Mo, "A superhydrophobic polyphenylene sulfide composite coating with anti-corrosion and self-cleaning properties for metal protection," *Colloids and Surfaces A: Physicochemical and Engineering Aspects*, vol. 648, p. 129152, 2022.

[5] C.-M. Deng, Y. Zhu, S. Sun, J. Wei, and D.-H. Xia, "Analysis of failure causes of epoxy-phenolic coated tinplate after boiling sterilization," *Engineering Failure Analysis*, vol. 135, p. 106129, 2022.

[6] L. Guo, H. Wang, X. Li, G. Fei, Y. Yuan, and Y. Li, "A synergistic system of polyaniline@ graphene-alkyd resin via a Gemini surfactant for enhanced anti-corrosion properties," *Progress in Organic Coatings*, vol. 170, p. 106944, 2022.

[7] A. Marotta, N. Faggio, V. Ambrogi, A. Mija, G. Gentile, and P. Cerruti, "Biobased furan-based epoxy/TiO_2 nanocomposites for the preparation of coatings with improved chemical resistance," *Chemical Engineering Journal*, vol. 406, p. 127107, 2021

[8] W. Liu, Z. Mo, C. Shuai, S. He, R. Yue, X. Guo, Y. Chen, H. Zheng, J. Zhu, R. Guo, and N. Liu, "Fabrication of TiO_2/CeO_2/PPS corrosion protective hydrophobic coating by air spraying," *Colloids and Surfaces A: Physicochemical and Engineering Aspects*, vol. 647, p. 129056, 2022.

[9] S. Liu, H. Xe, Q. Cao, Y. Ning, Y. Song, C. Zhand, and B. Liu, "Preparation of a novel IPDI/PUF@CeO_2 bi-functional microcapsules and its improvement for the self-healing and anti-corrosion performance in epoxy coatings," *Progress in Organic Coatings*, vol. 169, p. 106897, 2022.

[10] E. Zumelzu, and C. Cabezas, "Observations on the influence of microstructure on electrolytic tinplate corrosion," *Materials Characterization*, vol. 34, no. 2, pp. 143-148, 1995.

[11] G. G. D. Nascimento, J. L. C. D. Santos, I. C. P. Margarit, and O. R. Mattos, "Lacquered tinplate: Corrosion resistance in the function of lacquering conditions," *Electrochimica Acta*, vol. 41, no. 7-8, pp. 1099-1102, 1996.

[12] D. H. Xia, J. H. Wang, S. Z. Song, B. Zhong, and Z. W. Han, "The corrosion behavior of lacquered tinplate in functional beverage," *Advanced Materials Research*, vol. 233-235, pp. 1747-1751, 2011.

[13] J. E. Charbonneau, "Recent case histories of food product -metal container interactions using scanning electron microscopy-x-ray microanalysis," *Scanning*, vol. 19, no. 7, pp. 512-518, 1997.

[14] X. Huang, N. Li, L. Cao, and J. Zheng, "Electrodeposited lanthanum film as chromate replacement for tinplate," *Materials Letters*, vol. 62, no. 3, pp. 466-469, 2008.

[15] B. X. Huang, P. Tornatore, and Y.-S. Li, "IR and Raman spectroelectrochemical studies of corrosion films on tin," *Electrochimica Acta*, vol. 46, no. 5, pp. 671-679, 2001.

[16] A. N. Grassino, Z. Grabarić, A. Pezzani, G. Squitieri, and K. Berković, "Corrosion inhibition with different protective layers in tinplate cans for food preservation," *Journal of the Science of Food and Agriculture*, vol. 90, no. 14, pp. 2419-2426, 2010.

[17] R. Catalá, M. Alonso, R. Gavaram E. Almeida, J. Bastidas, J. M. Puente, and N. de Cristaforo,"Titanium-passivated tinplate for canning foods," *Food Science and Technology International*, vol. 11, no. 3, pp. 223-227, 2005.

[18] C. A. Gervasi, P. A. Palacios, M. v Fiori Bimbi, and P. E. Alvarez, "Electrochemical studies on the anodic behavior of tin in citrate buffer solutions," *Journal of Electroanalytical Chemistry*, vol. 639, no. 1-2, pp. 141-146, 2010.

[19] O. Hazzazi, "On the pitting corrosion behaviour of pure Al by halide ions in neutral sulphate solutions and the effect of some inorganic inhibitors," *Journal of King Abdulaziz University-Science*, vol. 19, no. 1, pp. 47-65, 2007.

[20] G. W. Patrick, "Internal corrosion of tinplate food containers," *Anti-Corrosion Methods and Materials*, vol. 23, no. 6, pp. 9-11, 1976.

[21] A. S. Tselesh, "Anodic behaviour of tin in citrate solutions: The IR and XPS study on the composition of the passive layer," *Thin Solid Films*, vol. 516, no. 18, pp. 6253-6260, 2008.

[22] S. A. M. Refaey, and G. Schwitzgebel, "Electrochemical impedance spectroscopic investigation of dissolution, passivation and pitting corrosion of tin in Na_2CO_3 solution and the effect of Cl− and I− ions," *Applied Surface Science*, vol. 135, no. 1-4, pp. 243-253, 1998.

[23] M. Jafarian, F. Gobal, I. Danaee, R. Biabani, and M. G. Mahjani, "Electrochemical studies of the pitting corrosion of tin in citric acid solution containing Cl−," *Electrochimica Acta*, vol. 53, no. 13, pp. 4528-4536, 2008.

[24] G. Urbano, V. E. Reyes, M. A. Veloz, and I. González, "Pyrite–arsenopyrite galvanic interaction and electrochemical reactivity," *The Journal of Physical Chemistry C*, vol. 112, no. 28, pp. 10453-10461, 2008.